QED AND ELECTROWEAK CORRECTIONS TO DEEP INELASTIC SCATTERING*

D. BARDIN[a,b], J. BLÜMLEIN[a], PENKA CHRISTOVA[c,**]
LIDA KALINOVSKAYA[b] AND T. RIEMANN[a]

[a] DESY–Zeuthen, Platanenallee 6, D-15735 Zeuthen, Germany
[b] Bogoliubov Laboratory for Theoretical Physics,
JINR, ul. Joliot-Curie 6, RU–141980 Dubna, Russia
[c] Bishop Konstantin Preslavsky University of Shoumen,
9700 Shoumen, Bulgaria

(*Received January 14, 1997*)

We describe the state of the art in the field of radiative corrections for deep inelastic scattering. Different methods of calculation of radiative corrections are reviewed. Some new results for QED radiative corrections for polarized deep inelastic scattering at HERA are presented. A comparison of results obtained by the codes POLRAD and HECTOR is given for the kinematic regime of the HERMES experiment. Recent results on radiative corrections to deep inelastic scattering with tagged photons are briefly discussed.

PACS numbers: 12.20. Ds, 12.15. Lk

1. Introduction

The knowledge of QED, QCD, and electroweak (EW) radiative corrections (RC) to the different deep inelastic scattering (DIS) processes is indispensable for the precise determination of the nucleon structure functions (SF). The forthcoming high statistics measurements of unpolarized and polarized SF at H1, ZEUS, HERMES, and SLAC require the knowledge of the RC at the percent level. This has to be met by adequately precise theoretical calculations.

In this report we summarize the actual status in the field of RC's for DIS. In section 2, we present a short review of different methods used with an emphasis on the so-called Model Independent approach (MI). Here, we

* Presented at the Cracow International Symposium on Radiative Corrections to the Standard Model, Cracow, Poland, August 1–5, 1996.
** Supported by PECO contract ERBCIPDCT-94-0016.

also describe results of a recent new calculation [1] of the QED corrections for polarized DIS including both γ and Z-boson exchange and accounting for all twist-2 contributions to the polarized SF's for both longitudinally and transversely polarized nucleons. In section 3, we present some new numerical results of this calculation. Section 4 sketches briefly recent results on the RC's for DIS with tagged photons [2]. This report represents a natural continuation of a talk [3] presented at the Warsaw Rochester Conference. In that talk an additional motivation is presented showing why the field is still a very vivid one.

2. Different approaches

2.1. *A qualitative comparison of Monte Carlo, semi-analytic, and deterministic approaches*

Until recently, two basic approaches to the RC's for DIS were used:

- The Monte Carlo (MC) approach aims at the construction of precise event generators (MCEG). This approach is exclusive and deals with completely differential cross-sections. Therefore it is rather flexible with respect to experimental applications, *e.g.* allowing for cuts. MCEG are real tools for data analysis. In principle, this approach suffers of statistical errors although a very impressive performance of MCEG's has been reached in recent years, see [4] and [5]. Typical examples of MCEG's for DIS are: `HERACLES` [6], `LESKO-F` [7], and `KRONOS` [8].
- Semi-Analytic (SAN) approaches aim at partly integrated cross-sections. Therefore they are much less flexible concerning possible cuts as compared to MCEG's. Only a limited number of inclusive distributions can be usually evaluated and no event generation is possible. However, the method provides fast and precise codes, provide exact benchmarks for MCEG's. The underlying physics is clearly exhibited, and sometimes appealing formulae emerge as a reward. These are the reasons why people will probably always try to perform SAN calculations. Furthermore, SAN codes may be used for fitting of theory predictions to experimental data at the final phase of their analysis. Examples of SAN codes for DIS are: `HELIOS` [9], `TERAD91` [10], `FERRAD` [11, 12], `APHRODITES` [13], `POLRAD` [14] and finally `HECTOR` [15], to which this talk is largely related.

Recently people began to use the so-called *Deterministic Approach* (DA), see, for instance, [16]. The DA is an alternative to the MC approach but without the ability of event generation. It also operates with completely differential cross-sections but integrates avoiding MC methods. A faster computing than in the case of MC may emerge since the integration is based on methods possessing better convergency (see the talk by Ohl [17] in these proceedings for a discussion of basic issues of DA). A necessary feature of DA should be the access to **any** realistic experimental cuts. This is usually achieved by the explicit solution of the relevant kinematic inequalities for the phase space boundaries. The elements of the DA are used in two of our recent codes, *μela* `1.00` [18] and one of the new branches in `HECTOR 1.11` [19].

2.2. Model independent approach

The Model Independent approach to the problem under consideration is usually understood as the description of the QED RC's to **only** the leptonic line of the Born-level Feynman diagrams. The hadronic part of the diagrams is assumed to be untouched. Therefore both the Born approximation and the radiative diagrams contain the same *hadronic tensor* accessing hadron dynamics through a potentially *Model Independent* description by means of the *structure functions*. This is possible only for the neutral current (NC) DIS where a continuous flow of the electric charge through the leptonic line ensures the QED gauge invariance of the description to all orders. The MI approach was comprehensively reviewed in [20] recently.

2.2.1. Born cross-section for the process $ep \to eX$

Here we present a complete set of formulae for the polarized DIS Born cross-section which can be written as a contraction of leptonic ($L^{\mu\nu}$) and hadronic ($W_{\mu\nu}$) tensors:

$$d\sigma_{\text{BORN}} = \frac{2\pi\alpha^2}{Q^4} y \left[L^{\mu\nu} W_{\mu\nu} \right] dx dy, \tag{1}$$

with the usual notation for momentum transfer (q), the invariants (Q^2, S),

$$q = k_1 - k_2, \qquad Q^2 = -q^2 = -t, \qquad S = 2(p \cdot k_1), \tag{2}$$

and the Bjorken scaling variables (x, y)

$$x = \frac{Q^2}{Sy}, \qquad y = \frac{p \cdot q}{p \cdot k_1}. \tag{3}$$

The polarization of the lepton beam is described by the spin density matrix

$$\rho(k_1) = \sum_s u^s(k_1) \bar{u}^s(k_1) = \tfrac{1}{2} \left(1 - \gamma_5 \hat{\xi}_e\right) \left(\hat{k}_1 + m\right), \tag{4}$$

where ξ_e is the lepton polarization vector, satisfying

$$\xi_e \cdot k_1 = 0. \tag{5}$$

The **leptonic tensor** on the Born-level is derived straightforwardly

$$\begin{aligned} L^{\mu\nu} &= 2\left[k_1^\mu k_2^\nu + k_1^\nu k_2^\mu - g^{\mu\nu}(k_1\cdot k_2)\right] L_{\rm S}(Q^2) \\ &\quad +2ip_e k_{1\alpha} k_{2\beta}\varepsilon^{\alpha\beta\nu\mu} L_{\rm A}(Q^2). \end{aligned} \tag{6}$$

It contains a symmetric (S) and an antisymmetric (A) part

$$\begin{aligned} L_{\rm S}(Q^2) &= Q_e^2 + 2|Q_e|\left(v_e - p_e\lambda_e a_e\right)\chi(Q^2) \\ &\quad + \left(v_e^2 + a_e^2 - 2p_e\lambda_e v_e a_e\right)\chi^2(Q^2), \\ L_{\rm A}(Q^2) &= -p_e\lambda_e Q_e^2 + 2|Q_e|\left(a_e - p_e\lambda_e v_e\right)\chi(Q^2) \\ &\quad + \left(2v_e a_e - p_e\lambda_e\left(v_e^2 + a_e^2\right)\right)\chi^2(Q^2). \end{aligned} \tag{7}$$

In (7), v_e and a_e stand for the vector and axial-vector couplings of electrons to Z-boson, $p_e = 1$ for a particle beam and $p_e = -1$ for an antiparticle beam, $\chi(Q^2)$ is the γ/Z propagator ratio

$$\chi(Q^2) = \frac{G_\mu}{\sqrt{2}}\frac{M_Z^2}{8\pi\alpha}\frac{Q^2}{Q^2 + M_Z^2}. \tag{8}$$

The expression (6) possesses a nice factorization property when the tensorial structures decouple from γ and Z propagators and couplings. This is a consequence of the *Ultra Relativistic Approximation* (URA) for the longitudinal polarization of incoming leptons which implies

$$\xi_e = \frac{\lambda_e}{m}k_1. \tag{9}$$

This approximation is very accurate for the description of the Born cross-section since it results in neglecting of terms of $\mathcal{O}(m^2/Q^2)$. It is not precise enough, however, for the description of radiative polarized DIS, and as a result the factorization property (6) is lost.

The **hadronic tensor** is being constructed from general principles of invariance (Lorenz invariance, current conservation). There is no unique presentation for it in the literature. We use the form of Ref. [21], where one can also find a review of other presentations used:

$$
\begin{aligned}
W_{\mu\nu} &= p^0(2\pi)^6 \sum \int \langle p'|\mathcal{J}_\mu^{J_1}|p\rangle\langle p|\mathcal{J}_\nu^{J_2}|p'\rangle \delta^4(\sum_i p_i' - p') \prod_i dp_i' \\
&= \left(-g_{\mu\nu} + \frac{q_\mu q_\nu}{q^2}\right) F_1^{J_1 J_2}(x,Q^2) + \frac{\widehat{p_\mu}\widehat{p_\nu}}{p\cdot q} F_2^{J_1 J_2}(x,Q^2) \\
&\quad -ie_{\mu\nu\lambda\sigma}\frac{q^\lambda p^\sigma}{2p\cdot q} F_3^{J_1 J_2}(x,Q^2) + ie_{\mu\nu\lambda\sigma}\frac{q^\lambda s^\sigma}{p\cdot q} g_1^{J_1 J_2}(x,Q^2) \\
&\quad +ie_{\mu\nu\lambda\sigma}\frac{q^\lambda(p\cdot q s^\sigma - s\cdot q p^\sigma)}{(p\cdot q)^2} g_2^{J_1 J_2}(x,Q^2) \\
&\quad + \left[\frac{\widehat{p_\mu}\widehat{s_\nu} + \widehat{s_\mu}\widehat{p_\nu}}{2} - s\cdot q\frac{\widehat{p_\mu}\widehat{p_\nu}}{p\cdot q}\right]\frac{1}{p\cdot q} g_3^{J_1 J_2}(x,Q^2) \\
&\quad + s\cdot q\frac{\widehat{p_\mu}\widehat{p_\nu}}{(p\cdot q)^2} g_4^{J_1 J_2}(x,Q^2) + \left(-g_{\mu\nu} + \frac{q_\mu q_\nu}{q^2}\right)\frac{s\cdot q}{p\cdot q} g_5^{J_1 J_2}(x,Q^2),
\end{aligned}
\tag{10}
$$

with

$$
\widehat{p_\mu} = p_\mu - \frac{p\cdot q}{q^2} q_\mu , \qquad \widehat{s_\mu} = s_\mu - \frac{s\cdot q}{q^2} q_\mu , \tag{11}
$$

and s is the four-vector of the nucleon spin. In the nucleon rest frame one has

$$
s = \lambda_p M(0,\vec{n}) . \tag{12}
$$

The hadronic structure functions $F_i^{J_1 J_2}$ and $g_i^{J_1 J_2}$ are associated with the respective currents $J_1, J_2 = \gamma, Z$.

Contracting the leptonic and hadronic tensors in (1), one derives the three Born cross-sections, depending on the nucleon spin orientation. The unpolarized DIS Born cross-section reads

$$
\frac{d\sigma^{\mathrm{U}}_{\mathrm{BORN}}}{dx dy} = \frac{2\pi\alpha^2}{Q^4}\sum_{i=1}^{3} S_i^{\mathrm{U}}(y,Q^2)\mathcal{F}_i(x,Q^2) , \tag{13}
$$

with the kinematical factors

$$
\begin{aligned}
S_1^{\mathrm{U}}(y,Q^2) &= 2yQ^2, \\
S_2^{\mathrm{U}}(y,Q^2) &= 2\left[S(1-y) - xyM^2\right], \\
S_3^{\mathrm{U}}(y,Q^2) &= (2-y)Q^2.
\end{aligned}
\tag{14}
$$

The two polarized DIS Born cross-sections are

$$\frac{d\sigma^{\mathrm{L,T}}_{\mathrm{BORN}}}{dx_l dy} = \frac{2\pi\alpha^2}{Q^4} f^{\mathrm{L,T}} \sum_{i=1}^{5} S^{\mathrm{L,T}}_{gi}(y,Q^2)\mathcal{G}_i(x,Q^2), \tag{15}$$

where

$$\begin{aligned} f^{\mathrm{L}} &= \lambda^{\mathrm{L}}_p, \\ f^{\mathrm{T}} &= \lambda^{\mathrm{T}}_p \cos\varphi \, \frac{d\varphi}{2\pi}\sqrt{\frac{4M^2x}{Sy}\left(1-y-\frac{M^2Q^2}{S^2}\right)}, \end{aligned} \tag{16}$$

and $S^{\mathrm{L,T}}_{g1-g5}(y,Q^2)$ are kinematical factors which obey a compact explicit form similar to (14), see Ref. [1].
The square root in (16) is related to the electron scattering angle θ_2:

$$\sqrt{\frac{4M^2x}{Sy}\left(1-y-\frac{M^2Q^2}{S^2}\right)} = \frac{1-y}{y}\sin\theta_2. \tag{17}$$

The angle φ is an azimuthal angle between transverse spin vectors and reaction plane. The nucleon polarization vector in (12) was taken as

$$\vec{n} = \lambda^{L}_p \frac{\vec{k}_1}{|\vec{k}_1|} \tag{18}$$

for the longitudinal case, and as

$$\vec{n} = \lambda^{T}_p \vec{n}_\perp \tag{19}$$

for the transverse case, where $\vec{n}_\perp$ satisfies

$$\vec{k_1}\cdot\vec{n}_\perp = 0. \tag{20}$$

The expressions (13) and (15) possess the same factorization property as leptonic tensor (6) does. As a consequence of it, the SF's combine with the γ and Z propagators and coupling constants and factor out from the universal kinematic factors, $S^{\mathrm{U,L,T}}_{F_i,g_j}$, which are simple functions of the two independent invariants, taken as y and Q^2 for definiteness.

The SF's $F_i^{J_1J_2}$ and $g_i^{J_1J_2}$ enter actually in only two combinations which are due to only two factorizing scalar structures, L_{S} and L_{A}, in (6). They are sometimes called *generalized* or *combined* SF's and read

$$
\begin{aligned}
\mathcal{F}_{1,2}(x,Q^2) &= Q_e^2 F_{1,2}^{\gamma\gamma}(x,Q^2) \\
&+2|Q_e|\left(v_e - p_e\lambda_e a_e\right)\chi(Q^2)F_{1,2}^{\gamma Z}(x,Q^2) \\
&+\left(v_e^2+a_e^2-2p_e\lambda_e v_e a_e\right)\chi^2(Q^2)F_{1,2}^{ZZ}(x,Q^2), \\
\mathcal{F}_3(x,Q^2) &= p_e\Biggl\{2|Q_e|\left(a_e - p_e\lambda_e v_e\right)\chi(Q^2)F_3^{\gamma Z}(x,Q^2) \\
&+\left[2v_e a_e - p_e\lambda_e\left(v_e^2+a_e^2\right)\right]\chi^2(Q^2)F_3^{ZZ}(x,Q^2)\Biggr\}, \\
\mathcal{G}_{1,2}(x,Q^2) &= p_e\Biggl\{-Q_e^2 p_e\lambda_e g_{1,2}^{\gamma\gamma}(x,Q^2) \\
&+2|Q_e|\left(a_e - p_e\lambda_e v_e\right)\chi(Q^2)g_{1,2}^{\gamma Z}(x,Q^2) \\
&+\left[2v_e a_e - p_e\lambda_e\left(v_e^2+a_e^2\right)\right]\chi^2(Q^2)g_{1,2}^{ZZ}(x,Q^2)\Biggr\}, \\
\mathcal{G}_{3,4,5}(x,Q^2) &= 2|Q_e|\left(v_e - p_e\lambda_e a_e\right)\chi(Q^2)g_{3,4,5}^{\gamma Z}(x,Q^2) \\
&+\left(v_e^2+a_e^2-2p_e\lambda_e v_e a_e\right)\chi^2(Q^2)g_{3,4,5}^{ZZ}(x,Q^2). \qquad (21)
\end{aligned}
$$

Eqs. (13)–(21) represent the complete set of formulae for the unpolarized and polarized DIS in the Born approximation. Now we turn to the first order QED RC's within MI approach.

2.2.2. Radiative process $ep \to eX\gamma$

For the description of the radiative process $ep \to eX\gamma$, one has to distinguish *leptonic* and *hadronic* variables:

$$
\begin{aligned}
q_l &= k_1 - k_2, & q_h &= p' - p, \\
Q_l^2 &= -q_l^2, & Q_h^2 &= -q_h^2, \\
y_l &= \frac{2p\cdot q_l}{S}, & y_h &= \frac{2p\cdot q_h}{S}. \qquad (22)
\end{aligned}
$$

Four invariants, y_l, Q_l^2, y_h, Q_h^2, together with an azimuthal angle φ_k varying from 0 to 2π (see [20] for a complete description of the kinematics of the process $ep \to eX\gamma$), form a complete set of five independent kinematic variables.

The differential cross-section for the scattering of polarized electrons off polarized protons, originating from the four bremsstrahlung diagrams (for both γ and Z-boson exchanges) has a form similar to (1)

$$\frac{d\sigma_{\rm BREM}}{dx_l dy_l} = 2\alpha^3 \int dy_h dQ_h^2 \frac{1}{Q_h^4} \left[\frac{1}{2\pi} \frac{d\varphi_k}{\sqrt{\lambda_q}} \frac{Sy_l}{4} \left(L^{\mu\nu}_{\rm RAD} W_{\mu\nu} \right) \right], \qquad (23)$$

with

$$\lambda_q \;=\; S^2 y_l^2 + 4M^2 Q_l^2. \qquad (24)$$

Here $W_{\mu\nu}$ is given by the same formulae (10)–(12) as for the Born case but now with all 4-momenta acquiring an index h, which stands for *hadronic* variables. This is a property of the MI approach. The quantity $L^{\mu\nu}_{\rm RAD}$ denotes the **leptonic radiative tensor**, an analog of the Born leptonic tensor (6), but for four bremsstrahlung diagrams. Its explicit form is presented in [1]. It does not exhibit such a simple factorizing structure as (6), see below. The unpolarized cross-section reads

$$\frac{d\sigma^{\rm U}_{\rm BREM}}{dx_l dy_l} = 2\alpha^3 \int dy_h dQ_h^2 \frac{1}{Q_h^4} \sum_{i=1}^{3} S_i^{\rm U}(y_l, Q_l^2, y_h, Q_h^2) \mathcal{F}_i(x_h, Q_h^2)\,. \qquad (25)$$

The explicit form of the kinematic factors $S_i^{\rm U}$ is given by Eqs. (3.14)– (3.16) of Ref. [20]. They are analogs of the factors (14) for the case of bremsstrahlung. Due to this they are functions of four invariant variables (22) (they are assumed to be integrated over the angle φ_k). As is seen from (25), the factorization for the three generalized SF's is fulfilled for the unpolarized cross-section.

The polarized DIS bremsstrahlung cross-sections have a more complicated structure:

$$\begin{aligned}
\frac{d\sigma^{\rm L,T}_{\rm BREM}}{dx_l dy_l} \;=\; & 2\alpha^3 f^{\rm L,T} \int dy_h \frac{dQ_h^2}{Q_h^4} \Biggl\{ \sum_{i=1}^{5} S_{gi}^{\rm L,T}(y_l, Q_l^2, y_h, Q_h^2) \mathcal{G}_i(x_h, Q_h^2) \\
& + \lambda_e 2m^2 \frac{(B_1, 1)}{C_1^{3/2}} \Biggl[\sum_{i=1}^{2} \Biggl(\mathcal{S}_{vi}^{\rm L,T}(y_l, Q_l^2, y_h, Q_h^2) \mathcal{G}_i^v(x_h, Q_h^2) \\
& + \mathcal{S}_{ai}^{\rm L,T}(y_l, Q_l^2, y_h, Q_h^2) \mathcal{G}_i^a(x_h, Q_h^2) \Biggr) \\
& + \sum_{i=3}^{5} \mathcal{S}_{zi}^{\rm L,T}(y_l, Q_l^2, y_h, Q_h^2) \mathcal{G}_i^z(x_h, Q_h^2) \Biggr] \Biggr\}. \qquad (26)
\end{aligned}$$

We note that the first sum in (26) exhibits the same factorization property as (25), but now for five polarized SF's. There also appear seven new generalized SF's, $\mathcal{G}_i^{v,a,z}(x_h, Q_h^2)$, and seven associated kinematic factors, $\mathcal{S}^{\rm L,T}_{vi,ai,zi}$. All these non-factorizable terms are proportional to λ_e and

m^2. These contributions turn out to be rather important since after one integration more they yield terms of $\mathcal{O}(1)$[1].

The additional generalized SF's are:

$$\begin{aligned}
\mathcal{G}^v_{1,2}(x,Q^2) &= Q_e^2 g^{\gamma\gamma}_{1,2}(x,Q^2) \\
&\quad +2|Q_e|v_e\chi(Q^2)g^{\gamma Z}_{1,2}(x,Q^2) + v_e^2\chi^2(Q^2)g^{ZZ}_{1,2}(x,Q^2), \\
\mathcal{G}^a_{1,2}(x,Q^2) &= a_e^2\chi^2(Q^2)g^{ZZ}_{1,2}(x,Q^2), \\
\mathcal{G}^z_{3,4,5}(x,Q^2) &= |Q_e|a_e\chi(Q^2)g^{\gamma Z}_{3,4,5}(x,Q^2) + v_e a_e\chi^2(Q^2)g^{ZZ}_{3,4,5}(x,Q^2). \quad (27)
\end{aligned}$$

All kinematic factors $S^{\mathrm{L,T}}_{gi}$ and $\mathcal{S}^{\mathrm{L,T}}_{vi,ai,zi}$ are of comparable complexity to those for the unpolarized DIS. They all were explicitly derived in [1]. The expressions for $B_{1,2}$ and $C_{1,2}$ are given in [20], Eqs. (A.30)–(A.31).

2.2.3. The net radiative correction

In all figures we show the dimensionless radiative correction factor:

$$\delta^k_l \equiv \delta^k(x_l,y_l) = \frac{d^2\sigma^k_{\mathrm{RAD}}/dx_l dy_l}{d^2\sigma^k_{\mathrm{BORN}}/dx_l dy_l} - 1, \tag{28}$$

where $d^2\sigma^k_{\mathrm{BORN}}$ is the Born cross-section for DIS and $d^2\sigma^k_{\mathrm{RAD}}$ is the *radiatively corrected* cross-section. The index k runs over *unpolarized*, *longitudinal* and *transverse* configurations. The cross-section $d^2\sigma^k_{\mathrm{RAD}}$ is usually presented as the sum of two terms:

$$\frac{d^2\sigma^k_{\mathrm{RAD}}}{dx_l dy_l} = \left[1+\frac{\alpha}{\pi}\,\delta_{\mathrm{VR}}(x_l,y_l)\right]\frac{d^2\sigma^k_{\mathrm{BORN}}}{dx_l dy_l} + \frac{d^2\sigma^k_{\mathrm{R}}}{dx_l dy_l}. \tag{29}$$

The first term contains the *universal, factorized correction*, originating from the *vertex* diagram and an IR-divergent part of the bremsstrahlung contribution. In *leptonic* variables it is given by Eq. (4.45) of [20]. The second *nonuniversal, non-factorized* term originates from the rest of bremsstrahlung contributions, which are free of IR-divergences by construction:

$$\begin{aligned}
\frac{d^2\sigma^k_{\mathrm{R}}}{dx_l dy_l} = 2\alpha^3 \int dy_h dQ_h^2 \Bigg[&\frac{1}{Q_h^4}\sum_i \mathcal{S}^k_i(y_l,Q_l^2,y_h,Q_h^2)\mathcal{F}^k_i(x_h,Q_h^2) \\
&-\frac{1}{Q_l^4}\sum_{i'} \mathcal{S}^k_{i'_{\mathrm{BORN}}}(y_l,Q_l^2)\mathcal{L}^{\mathrm{IR}}(y_l,Q_l^2,y_h,Q_h^2)\mathcal{F}^k_{i'}(x_l,Q_l^2)\Bigg],
\end{aligned} \tag{30}$$

where $\mathcal{L}^{\mathrm{IR}}(y_l,Q_l^2,y_h,Q_h^2)$ is given by Eq.(5.4) of [20].

[1] In the notation of Ref. [20], these are terms of $\mathcal{O}(m^2/z_1^2)$, which are known to give a non-negligible contribution in complete $\mathcal{O}(\alpha)$ calculations.

In (30), the indices i, i' run over the set of kinematical factors and generalized SF's $\mathcal{F}$ or $\mathcal{G}$ relevant to the index k. We note that all "additional" terms in (26) of $\mathcal{O}(m^2)$ are infrared finite. Therefore, they need not be subtracted in (30). Due to this one has two different indices i, i' running in different limits.

The formulae of this subsection, together with all kinematical factors being not given here, present a complete set of formulae for the MI approach to the RC's for polarized DIS. Here the presentation follows the spirit of the review [20].

2.3. *Leading logarithmic approximation*

In the leading logarithmic approximation (LLA), the $\mathcal{O}(\alpha)$ corrections consist of three incoherent contributions due to initial and final state radiations (ISR and FSR) [22–24] and the Compton peak [12, 25, 26]

$$\frac{d^2\sigma_{\text{RAD}}}{dxdy} = \frac{d^2\sigma_i}{dxdy} + \frac{d^2\sigma_f}{dxdy} + \frac{d^2\sigma_{\text{COMP}}}{dxdy}. \tag{31}$$

The ISR and FSR cross-sections have a similar generic structure:

$$\begin{aligned} \frac{d^2\sigma^{k,a}_{i,f}}{dxdy} &= \frac{\alpha}{2\pi}\left(\ln\frac{Q_a^2}{m^2} - 1\right)\int\limits_0^1 dz\frac{1+z^2}{1-z} \\ &\times\left\{\theta(z-z_0)\mathcal{J}\left.\frac{d^2\sigma^k_{\text{BORN}}}{dxdy}\right|^{a;i,f}_{x=\hat{x},y=\hat{y},S=\hat{S}} - \frac{d^2\sigma^k_{\text{BORN}}}{dxdy}\right\}, \\ \hat{x} &= \frac{\hat{Q}^2}{\hat{y}\hat{S}}, \quad \mathcal{J} \equiv \mathcal{J}(x,y,Q^2) = \left|\frac{\partial(\hat{x},\hat{y})}{\partial(x,y)}\right|. \end{aligned} \tag{32}$$

The lower integration boundary z_0 derives from the conditions

$$\hat{x}(z_0) \le 1, \qquad \hat{y}(z_0) \le 1. \tag{33}$$

Here the new index a stands for the different types of measurements, for which the definitions of the $\hat{x}$, $\hat{y}$, $\hat{S}$, as well as of the z_0, are known to be different (see for example [15]). Formulae of similar structure are known in the second order LLA, $\mathcal{O}((\alpha L)^2)$ [27].

For leptonic variables all the Compton contributions are known [1]:

$$\frac{d^2\sigma^{\text{U}}_{\text{COMP}}}{dx_l dy_l} = \frac{\alpha^3}{Sx_l^2}\frac{Y_+}{y_{l_1}}\int\limits_{x_l}^1\frac{dx_h}{x_h}\int\limits_{(Q_h^2)^{\min}}^{(Q_h^2)^{\max}}\frac{dQ_h^2}{Q_h^2}\Big[Z_+F_2^{\gamma\gamma}(x_h,Q_h^2)$$

$$
\left. - \left(\frac{x_l}{x_h}\right)^2 F_L^{\gamma\gamma}(x_h, Q_h^2)\right],
$$

$$
\frac{d^2\sigma^L_{\rm COMP}}{dx_l dy_l} = \left(-2\lambda_e\lambda_p^L\right)\frac{\alpha^3}{Sx_l^2}\frac{Y_-}{y_{l_1}}\int\limits_{x_l}^{1} dx_h \int\limits_{(Q_h^2)^{\min}}^{(Q_h^2)^{\max}} \frac{dQ_h^2}{Q_h^2} Z_- g_1^{\gamma\gamma}(x_h, Q_h^2),
$$

$$
\begin{aligned}
\frac{d^2\sigma^T_{\rm COMP}}{dx_l dy_l} &= \left(-2\lambda_e\lambda_p^T\right)\frac{\alpha^3}{Sx_l^2}\cos\varphi\frac{d\varphi}{2\pi}\frac{y_l}{y_{l_1}^2}\sqrt{\frac{4M^2x_l}{Sy_l}}\left(y_{l_1} - \frac{M^2x_ly_l}{S}\right) \\
&\times \int\limits_{x_l}^{1} dx_h \int\limits_{(Q_h^2)^{\min}}^{(Q_h^2)^{\max}} \frac{dQ_h^2}{Q_h^2}\Big\{ (Y_- - y_l z)\, z g_1^{\gamma\gamma}(x_h, Q_h^2) \\
&+2\left[Y_+ (1-z) + y_{l_1}\right] g_2^{\gamma\gamma}(x_h, Q_h^2), \Big\},
\end{aligned} \tag{34}
$$

where

$$
\begin{aligned}
Y_\pm &= 1 \pm y_{l_1}^2, \quad & Z_\pm &= \left[1 \pm (1-z)^2\right], \\
y_{l_1} &= 1 - y_l, & z &= \frac{x_l}{x_h}.
\end{aligned} \tag{35}
$$

The LLA formulae are remarkably compact. To derive the ISR and FSR contributions one has to know only the Born cross-section. No more complex are also the relations for the Compton peak contributions. A natural question arises: How precise are they as compared to complete $\mathcal{O}(\alpha)$ calculations? We will present some figures with comparisons of LLA and complete calculations in Section 3.

2.4. QPM approach, EWRC

The only way to go beyond *leptonic* corrections is to give up the MI approach in favour of complete $\mathcal{O}(\alpha)$ calculations within the framework of the quark-parton model (QPM) approach where one can access the following RC's:

(1) The QED RC's to the leptonic current;

(2) The QED RC's to the quark current – a model of hadronic RC's;

(3) The interference of lepton and quark bremsstrahlung together with the corresponding $\gamma\gamma, \gamma Z, \gamma W$ boxes;

(4) The electroweak radiative corrections (EWRC).

If identical SF's are chosen, the QPM leptonic current QED corrections (1) should agree exactly with those calculated in the MI approach. However, there is no access in the MI approach to the corrections (2), (3), and (4). The EWRC (4) are usually taken into account using the language of *effective weak couplings.*

`HECTOR 1.00` [15] contains two QPM-based branches with complete $\mathcal{O}(\alpha)$ QED and EWRC's to:

- NC and CC DIS in *leptonic* variables [28];
- NC DIS in *mixed* variables [29].

3. Numerical results

In this section we present some numerical results obtained with an upgraded version of the `HECTOR` package [19] and present an updated comparison with the results obtained by the code `POLRAD15` [14].

For a brief description of main features of these codes as well as for some numerical results illustrating the comparison between LLA and complete $\mathcal{O}(\alpha)$ calculations, and for a first comparison of these two codes we refer the reader to [3] and [30].

In all numerical calculations we used the CTEQ3M parametrization [31] for the unpolarized SF's and the GRSV'96 parametrization [32] for the polarized SF's.

3.1. New results of LLA/complete comparison

In Figs. 1 and 2 a comparison of the RC factors (28) is shown. For the calculations we used the $\mathcal{O}(\alpha)$ QED formulae presented in subsections 2.2 and 2.3 of this report. In the LLA calculations, all the three contributions (31) were used. We note that taking into account the Compton peak contribution in the form of the twofold integral (34) with a tuned upper limit $(Q^2_h)^{\max}$ (see [1] for details) improves substantially the agreement as compared to the case when only initial and final state RC (32) were considered.

An agreement at the same level of precision persists even if a cut on the invariant mass of the final hadronic state, M^2_h, or on the transfer momentum, Q^2_h, of the order of 100 GeV^2 is imposed.

We would like to warn the reader, however, that taking into account LLA alone is *not* fully sufficient in all cases. In particular, at HERMES energies the agreement becomes poorer, see Figs. 3 and 4 below, and even worse when rather loose cuts are imposed.

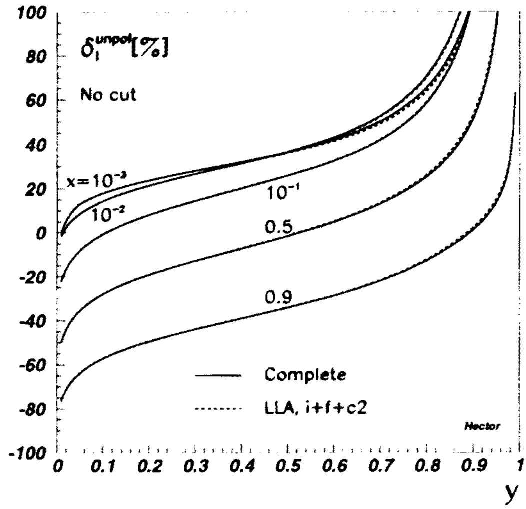

Fig. 1. A comparison of complete and LLA RC's at HERA collider kinematic regime for NC *unpolarized* DIS in *leptonic* variables.

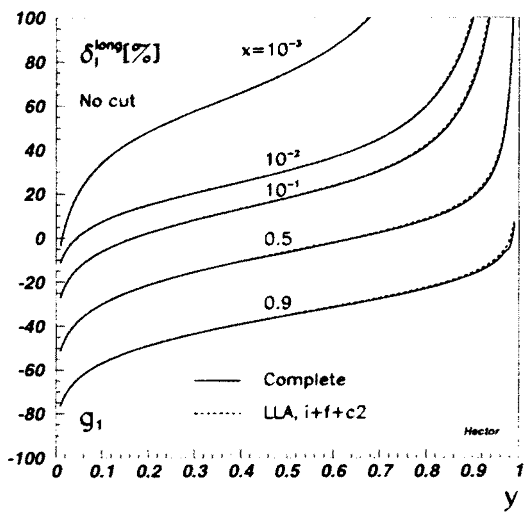

Fig. 2. The same as Figure 1 but for *longitudinal* DIS.

3.2. An updated comparison of HECTOR 1.11 *and* POLRAD15 *results*

This comparison, like the previous one, was done for the kinematic range of HERMES, for the leptonic measurement of polarized DIS on a proton target both for longitudinal and transverse orientations of the proton spin. Only the γ exchange diagrams and the first order QED RC's were retained.

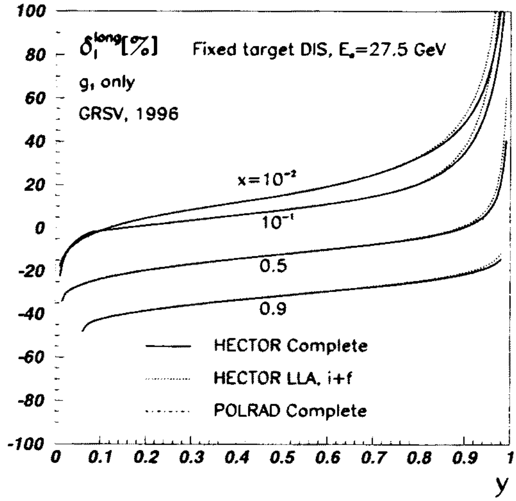

Fig. 3. A comparison of RC's calculated by **HECTOR** and **POLRAD** for NC *longitudinal* DIS in *leptonic* variables.

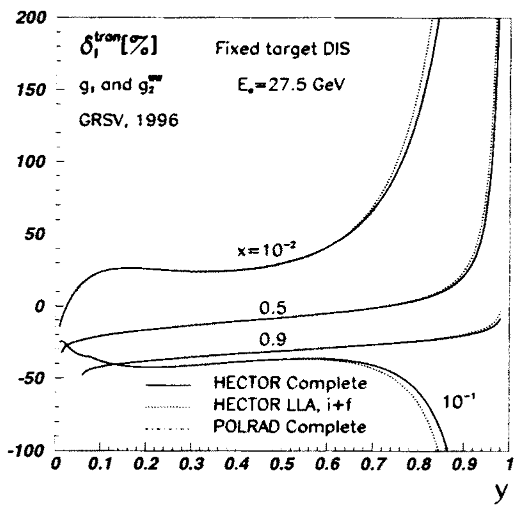

Fig. 4. The same as Figure 3 but for *transverse* DIS. For g_2 the Wandzura–Wilczek relation [33] was used.

Figures 3 and 4 update corresponding figures of [3] and [30]. These figures, together with a figure from Ref. [30] for the unpolarized DIS, demonstrate a very good agreement of the results of the "tuned" (*i.e.* with exactly the same, simplified input) comparison between `HECTOR 1.11` and

POLRAD15. This does not replace future comparisons in the real experimental applications. The previously registered small disagreement for the polarized cases for low x and high y was due to the omission of terms of $\mathcal{O}(m^2)$ in Eq. (26) in [3] and [30].

From figures 3 and 4 one can also see how well the LLA and complete calculations do agree at HERMES energies.

4. RC for tagged photon DIS

The interest to DIS with *tagged photons* arose recently. The H1 and ZEUS collaborations collected samples of DIS events in which a photon is observed in the so-called backward luminosity tagger with a typical angular acceptance of 0.5 mrad around the beam axis. Although the present statistics is limited to several thousand events, it will largely improve with more HERA data coming. This is the reason why the RC to this sample have to be calculated at the percent level of precision. The relevant DIS Born-level cross-section, instead of (13), is described by a three fold-differential expression

$$\frac{d^3\sigma_{\mathrm{BREM}}}{dx_l dy_l dE_\gamma} = \frac{2\alpha^3}{\pi} y_l \int d\cos\theta_\gamma \int d\varphi_\gamma \frac{E_\gamma}{Q_h^4} \sum_{i=1}^{3} S_i^{\mathrm{U}} \mathcal{F}_i, \tag{36}$$

where the integration is performed over the angular range covered by the photon tagger. In (36) the kinematic factors S_i^{U}, contrary to (25), are understood to be completely differential in five kinematic variables. The latter are chosen as x_l, y_l, and θ_γ, φ_γ, E_γ in the laboratory frame, where the photon variable cuts are defined. We note that the usual definitions of x_l and y_l (22) are used in this section, *i.e.* they are not recalculated using the *reduced* electron beam energy.

In a recent paper [2], we performed a detailed calculation of the Born cross-section (36) and an evaluation of the RC to it. The main idea is to combine the MI approach for the description of the Born cross-section (25) (the DIS bremsstrahlung is the Born-level process in the problem under consideration) with the LLA for the description of ISR QED corrections (32).

In figures 5 and 6 we show the Born cross-section and the RC for $E_\gamma = 5$ GeV, the peak value of the distribution of tagged DIS events.

The RC exhibits nice properties: it shows a typical behaviour in soft and hard bremsstrahlung corners in y and is quite flat in between. In the plateau region, its value is limited within a $\pm 10\%$ band. The RC grows slightly with increasing E_γ, *e.g.* for $E_\gamma = 10$ GeV the plateau behaviour becomes less pronounced and for reasonable x_l and y_l (*e.g.* $y_l < 0.9$) its value is limited within a $+5\%, +25\%$ interval.

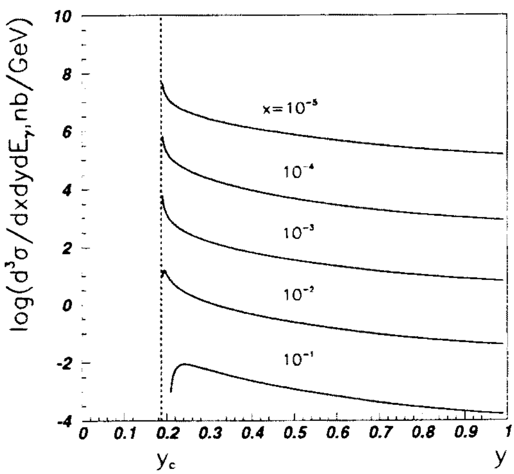

Fig. 5. The threefold differential Born DIS cross-section with *tagged photons* for $E_\gamma = 5$ GeV; $y_c = E_\gamma / E_e$, $E_e = 27.5$ GeV.

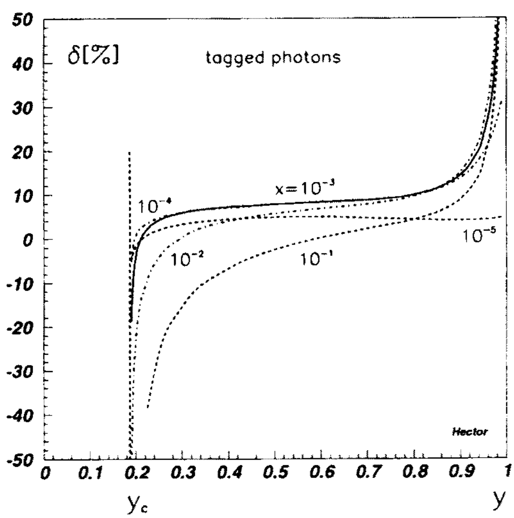

Fig. 6. The RC to DIS cross-section with *tagged photons*.

The fact that the RC's for DIS with tagged photons are not so big gives reasons to trust a simplified approach as used here. However, a complete calculation of $\mathcal{O}(\alpha)$ RC's to the DIS bremsstrahlung cross-section seems to be still an important physical task in view of high statistics data to be taken at HERA in the coming years.

The authors are very much obliged to I. Akushevich for fruitful collaboration on the comparison with POLRAD and for important remarks. We are thankful to A. Arbuzov for an enjoyable common work within the HECTOR project. We are grateful to M. Klein for reading of the manuscript.

REFERENCES

[1] D. Bardin, J. Blümlein, P. Christova, L. Kalinovskaya, DESY 96–189.

[2] D. Bardin, L. Kalinovskaya, T. Riemann, DESY 96–213.

[3] D. Bardin, to appear in Proceedings of 28th International Conference on High Energy Physics, 25-31 July 1996, Warsaw, Poland.

[4] S. Jadach, O. Nicrosini (conveners) *et al.*, Proceedings of the Workshop on Physics at LEP 2, eds., G. Altarelli, T. Sjöstrand, F. Zwirner, CERN Yellow Report CERN 96-01 (1996), **Vol. 2**, p.229.

[5] D. Bardin, R. Kleiss (conveners) *et al.*, Proceedings of the Workshop on Physics at LEP 2, eds., G. Altarelli, T. Sjöstrand, F. Zwirner, CERN Yellow Report CERN 96-01 (1996), **Vol. 2**, p.3.

[6] A. Kwiatkowski, H.-J. Möhring, H. Spiesberger, Proceedings of the Workshop on Physics at HERA, Oct. 29–30, 1991, Hamburg (DESY, Hamburg, 1992); W. Buchmüller, G. Ingelman (eds.), **Vol. 3**, p.1294; *Comput. Phys. Commun.* **69**, 155 (1992).

[7] S. Jadach, W. Placzek, Proceedings of the Workshop on Physics at HERA, Oct. 29–30, 1991, Hamburg (DESY, Hamburg, 1992); W. Buchmüller, G. Ingelman (eds.), **Vol. 3**, p. 1330.

[8] H. Anlauf, H.D. Dahmen, P. Manakos, T. Mannel, T. Ohl, Proceedings of the Workshop on Physics at HERA, Oct. 29–30, 1991, Hamburg (DESY, Hamburg, 1992); W. Buchmüller, G. Ingelman (eds.), **Vol. 3**, p.1311.

[9] J. Blümlein, Proceedings of the Workshop on Physics at HERA, Oct. 29–30, 1991, Hamburg (DESY, Hamburg, 1992); W. Buchmüller, G. Ingelman (eds.), **Vol. 3**, p.1270.

[10] A. Akhundov, D. Bardin, L. Kalinovskaya, T. Riemann, *ibid.* **Vol. 3**, p.1285.

[11] FORTRAN code FERRAD35 used by SMC and based on Ref. [12].

[12] L.W. Mo, Y.S. Tsai, *Rev. Mod. Phys.* **41**, 205 (1969).

[13] G. Montagna, O. Nicrosini, L. Viola, in: the same Proceedings as in Ref. [6], **Vol. 3**, p.1267.

[14] I. Akushevich, N. Shumeiko, *J. Phys.* **G20**, 513 (1994); I. Akushevich, A. Ilyichev, N. Shumeiko, *Yad. Fiz.* **58**, 2029 (1995).

[15] A. Arbuzov, D. Bardin, J. Blümlein, L. Kalinovskaya, T. Riemann, *Comput. Phys. Commun.* **94**, 128 (1996).

[16] G. Passarino, *Comput. Phys. Commun.* **97**, 261 (1996).

[17] T. Ohl, *Acta Phys. Pol.* **B28**, this issue; hep-ph/9610349.

[18] D. Bardin, L. Kalinovskaya, FORTRAN code μela 1.00.

[19] A. Arbuzov, D. Bardin, J. Blümlein, P. Christova, L. Kalinovskaya, T. Riemann, FORTRAN code HECTOR 1.11.

[20] A. Akhundov, D. Bardin, L. Kalinovskaya, T. Riemann, *Fortschr. Phys.* **44**, 373 (1996).

[21] J. Blümlein, N. Kochelev, *Phys. Lett.* **B381**, 296 (1996).

[22] A. De Rujula, R. Petronzio, A. Savoy-Navarro, *Nucl. Phys.* **B154**, 394 (1979); M. Consoli, M. Greco, *Nucl. Phys.* **B186**, 519 (1981); E. Kuraev, N. Merenkov, V. Fadin, *Sov. J. Nucl. Phys.* **47**, 1009 (1988).

[23] J. Blümlein, *Z. Phys.* **C47**, 89 (1990); *Phys. Lett.* **B271**, 267 (1991).

[24] I. Akushevich, T. Kukhto, *Yad. Fiz.* **52**, 1442 (1990); *Acta Phys. Pol.* **B22**, 771 (1991).

[25] J. Blümlein, G. Levman, H. Spiesberger, in: *Proceedings of the Workshop on Research Directions of the Decade, Snowmass 1990*, ed. E. Berger (World Sci., Singapore, 1992); *J. Phys.* **G19**, 1695 (1993).

[26] I. Akushevich, T. Kukhto, F. Pacheco, *J. Phys.* **G18**, 1737 (1992).

[27] J. Kripfganz, H. Möhring, H. Spiesberger, *Z. Phys.* **C49**, 501 (1991); J. Blümlein, *Z. Phys.* **C65**, 293 (1995).

[28] D. Bardin, C. Burdik, P. Christova, T. Riemann, *Z. Phys.* **C42**, 679 (1989); *Z. Phys.* **C44**, 149 (1989).

[29] D. Bardin, P. Christova, L. Kalinovskaya, T. Riemann, *Phys. Lett.* **B357**, 456 (1995).

[30] D. Bardin, J. Blümlein, P. Christova, L. Kalinovskaya, Preprint DESY 96–198, September 1996; in Proceedings of the Workshop "Future Physics at HERA", G. Ingelman, A. De Roeck, R. Klanner (eds.), **Vol. 1**, p. 13; hep-ph/9609399.

[31] H.L. Lai, J. Botts, J. Huston, J.G. Morfin, J.F. Owen, J.W. Qiu, W.K. Tung, H. Weerts, *Phys. Rev.* **D51**, 4763 (1995).

[32] M. Glück, E. Reya, M. Stratmann, W. Vogelsang, *Phys. Rev.* **D53**, 4775 (1996).

[33] S. Wandzura, F. Wilczek, *Phys. Lett.* **B72**, 195 (1977).